Finite-element simulation of multiaxial compaction of sponge titanium powder

Cite as: AIP Conference Proceedings **1785**, 040008 (2016); https://doi.org/10.1063/1.4967065
Published Online: 18 November 2016

Ivan Berezin, Anton Nesterenko, Alexander Zalazinsky, and Nikolay Michurov

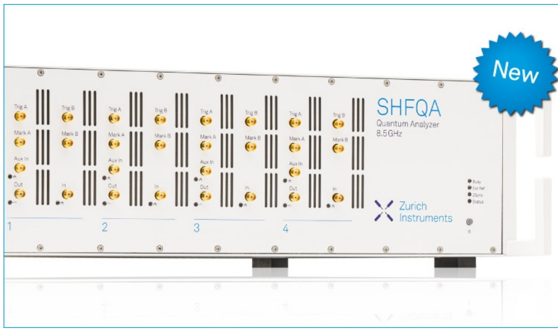

Finite-Element Simulation of Multiaxial Compaction of Sponge Titanium Powder

Ivan Berezin[1,2,a)], Anton Nesterenko[1,b)], Alexander Zalazinsky[1], Nikolay Michurov[1]

[1]*Institute of Engineering Science (IES), Ural Branch of the Russian Academy of Sciences, 34 Komsomolskaya St., Ekaterinburg, 620049, Russia. Tel.: (343) 375-35-90.*
[2]*Ural Federal University named after the first President of Russia B.N. Yeltsin, 19 Mira St., 620002, Ekaterinburg, Russia.*

[a)]Corresponding author: berezin@imach.uran.ru
[b)] nav@imach.uran.ru

Abstract. In this study, based on numerical simulation of multiaxial compaction process, an attempt is made to establish a consistent relation of material porosity to shearing and normal stresses under various stress state conditions. The finite element model of the multiaxial compression process has made it possible to apply both radial and axial pressures independently of one another. Powdered titanium sponge is modeled using the modified Drucker–Prager Cap plasticity model. A mathematical model of porosity alteration depending on the range of the equivalent pressure stress and the von Mises equivalent stress has been obtained. A comparison between finite-element simulation and experimental research on the die compaction of titanium sponge has been made.

INTRODUCTION

The intensification of the compaction metal powders significantly depends on the choice of an effective deformation scheme providing reduced compaction forces with the increasing density of the compacted material. It is known [1, 2] that the achievement of high densities of deformable porous solid is only possible in the processes that implement optimal combinations of normal and shear stresses. In this connection, one should expect that the problem of increasing the density of a workpiece may be solved on the basis of a complex analysis of the stressed state on compaction and on the improvement of existing load distribution schemes. At that, a correlation between compacting pressure and material density relate mostly to the deformation schemes for which they were obtained. Thus, the identification of a consistent pattern of changing the material density (porosity), depending on the value of shear and normal stress at various deformation schemes, is a relevant objective.

The most complete study of material densification may be based on the use of triaxal (multiaxial) compression machines [3, 4]. This type of experimental equipment provides different stress conditions in a workpiece by a possibility of independently applying both radial and axial pressures. The complexity of experiments and low effectiveness of triaxial compression equipment make this approach expensive and inefficient. This study presents a finite-element simulation of the process of multiaxial compression of sponge titanium powder for the purpose of identification of the quantitative pattern of material compaction depending on the combination of the equivalent pressure stress p and the von Mises equivalent stresses q.

FINITE-ELEMENT ANALISYS

Sponge titanium powder subjected to reversible thermo-hydrogen treatment was used [5]. Hydration has been carried out by thermal diffusion in a Sieverts-type vacuum machine up to 0.5 wt. % hydrogen concentration. At that,

Mechanics, Resource and Diagnostics of Materials and Structures (MRDMS-2016)
AIP Conf. Proc. 1785, 040008-1–040008-4; doi: 10.1063/1.4967065
Published by AIP Publishing. 978-0-7354-1447-1/$30.00

hydrogen alloying is temporary, and hydrogen is removed after plastic deformation by vacuum annealing. The granulometric composition corresponded to the particles sized from 2 mm to 5 mm.

The modified Drucker–Prager Cap plasticity model has been applied for the description of titanium sponge yield criterion. Figure 1 shows the scheme of the multiaxial compaction process.

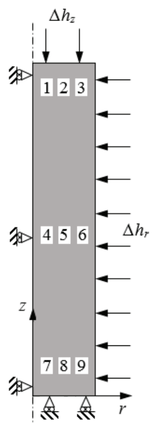

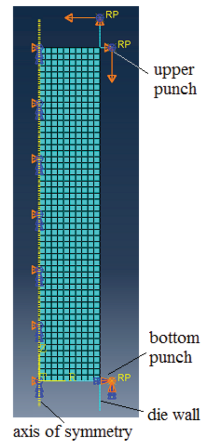

(a) (b)

FIGURE 1. Computational scheme (a) and the finite-element model (b)

At stage I, the workpiece was subjected to non-uniform multiaxial compression. The displacement values Δh_z and Δh_r were changed randomly, independently of one another, which made it possible to provide various schemes of the stress state and to identify the corresponding values of volumetric plastic strain ε^v_{pl}, the von Mises equivalent stresses q and the equivalent pressure stress p in areas No. 1–9 (see Fig.1a).

At stage II of the research, the workpiece was only subjected to axial compression by moving the upper punch to Δh_z with a fixed position of the die wall (Δh_r = const = 0). The deformation was stopped upon the achievement of the nonporous state in one of the workpiece areas. Stage III of experiments included the radial compression of the billet without axial punch movement (Δh_z = const = 0). The values of q, p and ε^v_{pl} were determined the same way as during the experiments at stages I and II.

RESULTS AND DISCUSSION

As a result of the finite-element simulation, the following mathematical model has been obtained:

$$\theta_{comp} = b_1 \cdot \exp\left(-b_2 \cdot k_q\right) + b_3 \cdot \exp\left(-b_4 \cdot k_p\right), \quad (1)$$

where θ_{comp} (%) is calculated material porosity, $k_q = q/q_s$, $k_p = p/q_s$, where q_s is the yield stress of material in the nonporous state. The coefficients involved in Eq. (1) have the following meanings: $b_1 = 6.222$; $b_2 = 1.585$; $b_3 = 43.21$; $b_4 = 1.142$. The graphic interpretation of Eq. (1) is presented in Fig. 2.

It is clear that the change in the value of equivalent pressure stress, expressed by the coefficient k_p, produces a more substantial effect on the compaction of the material as compared with shear deformation. Nevertheless, the absence of shear deformations in case of the stress condition of uniform isostatic compression ($k_q = 0$) does not allow achieving porosity below 6%. On the other hand, shear stresses ($k_p = 0$) alone do not lead to any substantial decrease in material porosity, whereas the change of θ_{comp} does not exceed 8 %. Consequently, the production of a quasimonolithic material with minimal porosity is only possible when there is the synchronizing action of hydrostatic and shearing deformations. When $k_q = 2$ and $k_p = 4$ are achieved, the porosity is close to zero and any further increase in k_q and k_p does not lead to any noticeable compaction of the material.

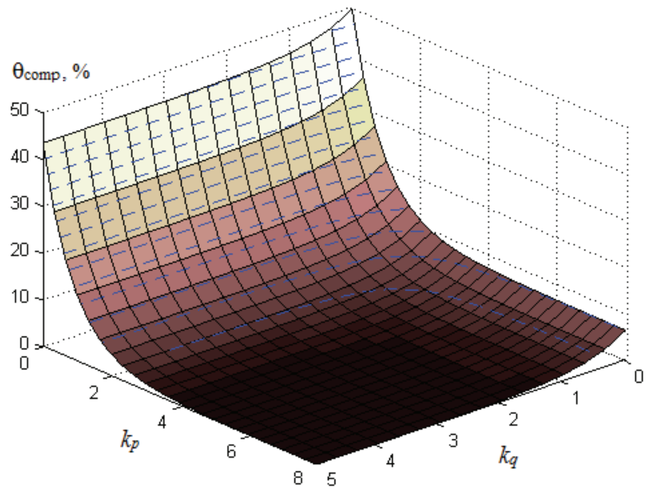

FIGURE 2. Calculated material porosity θ_{comp} (%) as dependent on the values of k_p and k_q

In order to verify Eq. (1) obtained from the finite-element simulation, die compaction of titanium sponge was experimentally studied. The workpieces were produced under a pressure of 1000 MPa on the upper punch and a temperature of 325 °C. In order to determine porosity, thin plates in various axial sections of workpieces were produced (Fig. 3).

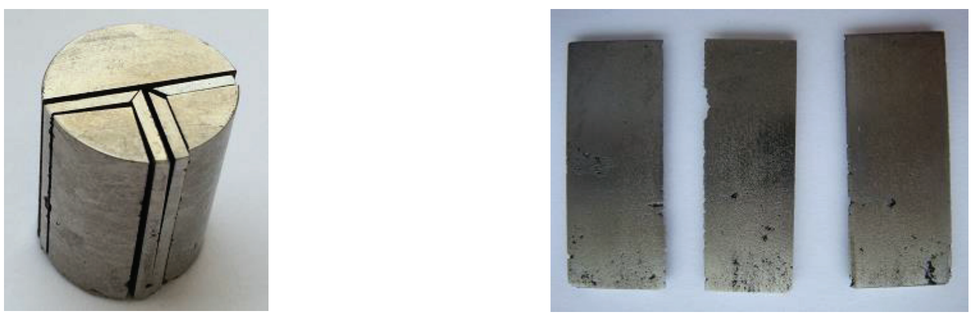

(a) (b)

FIGURE 3. A workpiece (a) and thin plates (b)

Figure 4 shows the microstructure of one of the thin plates, obtained on a Tescan Vega II XMU scanning electronic microscope. The actual dimensions of areas No. 1–9 are 1 mm height and 1 mm width. It is obvious that in the horizontal layer of the material, which is close to the upper punch, the porosity decreases from area 1 towards area 3. The consistency of the porosity distribution pattern in the material lying on the bottom of the container has an inverse dependence, as compaction occurs from area 9 towards area 7. In the vertical direction, the surface porosity of areas 1–3 is substantially lower than that of areas No 7–9. The porosity in various areas of the thin plate surfaces has been determined by quantitative metallography with the application of image processing and analysis with the use of the Matlab software. The statistical processing of the experimental data obtained after the quantitative evaluation of the microstructure was performed at the confidence level of 0.95. The method of maximal relative deviation has been used to verify the obtained data for the normality of distribution and elimination of gross errors.

The comparison of the simulation and experimental values of material porosity at points No. 1–9 is presented in Table 1. It is obvious that each of the nine points (corresponding to the column number in Table 1) of the workpiece section has unique strain-stress state characteristics. The most effective compaction is in area No. 3, where the von Mises equivalent stress acquires its maximum value $q = 794$ MPa and the equivalent pressure stress is the highest, $p = 526$ MPa. The lowest compaction, as expected, is in area No. 9, which is characterized by the lowest von Mises equivalent stress, $q = 257$ MPa, and by the value $p = 171$ MPa.

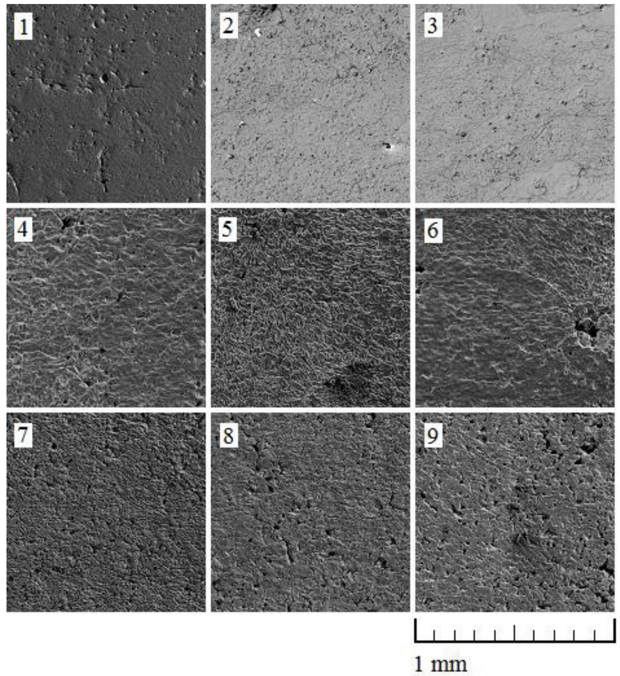

FIGURE 4. The microstructure of the thin plate surface in areas No. 1–9 (×166)

TABLE 1. Material porosity (θ) depending on the stress state characteristics (q, p) in areas No. 1–9

	Area No								
	1	**2**	**3**	**4**	**5**	**6**	**7**	**8**	**9**
q, MPa	576	617	794	519	539	564	494	444	257
p, MPa	384	413	526	347	356	368	324	290	171
θ_{exp}, %	1.32	0.82	0.60	1.96	1.73	1.34	2.18	2.84	5.90
θ_{comp}, %	0.80	0.59	0.18	1.18	1.08	0.95	1.50	2.14	7.47

CONCLUSION

The dependence of the variation of porosity on equivalent pressure stress and the von Mises equivalent stresses has been established from the numerical simulation of the process of multiaxial compression of titanium sponge. It has been found that equivalent pressure stress produces a more substantial effect on the compaction of material as compared to the effect of shear stress. It has been found that it is possible to produce materials with minimal porosity only when there is a joint action of normal and shear deformations. It has been shown that the consistency of the pattern of material porosity distribution corresponds to the regularity of changes in the field of equivalent pressure stress and the value of the von Mises equivalent stress, obtained by finite-element analysis.

REFERENCES

1. K. L. Nielsen, J. Dahl, V. Tvergaard, International Journal of Fracture **177**, 97 (2012).
2. V. Tvergaard, International Journal of Fracture **158**, 41 (2009).
3. P. Doremus, C. Geindreau, A. Marttin, L. Debove, R. Lecot, M. Dao, Powder Metallurgy **38**, 284 (1995).
4. H. Shin, J.B. Kim, S.J. Kim, K.Y. Rhee, Computational Materials Science **100**, 31 (2015).
5. A. V. Nesterenko, V. I. Novozhonov, A. G. Zalazinskii, A. V. Skripov, Russian Journal of Non-Ferrous Metals **56**, 287 (2015).